Using of Finite Element Method and Computational Analysis of Mechanical Properties of Stent-grafts

Stepan Major, Marie Hubalovska

***Abstract*—**The paper presents process of modeling and simulation as one of the most important method in current research in the area of biotechnological engineering. The paper focuses on implementation of the finite element method (FEM) as basis for creation of computer simulation model of mechanical properties of tubular laser cut stents. The FEM was applied for computational analysis and representation of dependence of the radial forces as functions of displacement and compressed stent diameter of two stent materials (Nitinol-49 and Nitinol-55) in different stent geometry. The simulation models created in SolidWorks® Simulation program were validated by experimental measured data and confirm good agreement.

***Keywords*—**Stent, Nitinol, Finite Element Method, Computer Simulation, Modeling, Biotechnological Engineering.

I. Introduction

Stents are narrow tubes. Production material of stents are wires or laser-cut tubes. The stents made by laser cutting are tubular meshes. The stent-grafts are inserted into arteries to help to keep them open so that blood can flow properly. The stent is mounted on a balloon catheter and delivered to the site of blockage. Endovascular aneurysm repair has clear benefits when compared with conventional open surgery in terms of lower trauma, earlier return to daily activities, reduced mortality, and lower morbidity. However, stent-graft failure, i.e., implant migration, device fatigue, and endoleaks resulting potentially are dangerous to patients life, therefore they are major concern [1, 2, 3].

II. Theoretical Background

A. Stent-graft Geometry

The geometry of the cross sections of studied stents is shown on the figure 1. The most analysis described in papers [1, 2, 3] study behavior only stents with simple geometry of type diamond and bridge-to bridge.

Figure 2 shows a stent-graft with 6 cells in 11 rows, e.g. a total of 66 cells built into the tubular stent. Figure 2 shows detailed view on stent with B geometry. Stent-grafts are composed from two different parts: stent and graft. Stent represents tubular structure which keeps the vein expanded, while the graft is covering the pipe. Stents are produced either by bonding wire or by laser cutting from tubes of small diameter. This diameter matches to diameter of crimpled or compressed stent-graft.

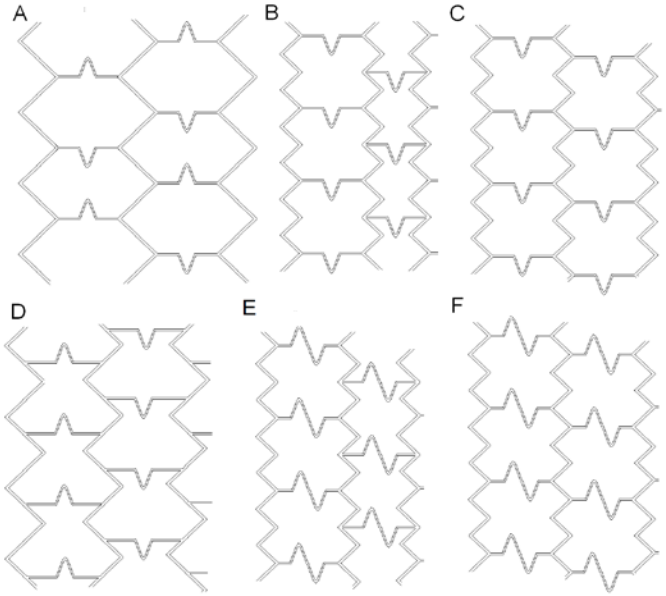

Fig. 1 A-F Different geometries of stent–graft.

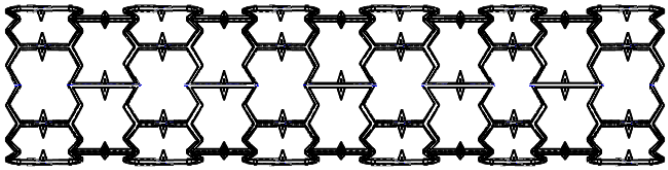

Fig. 2 Stent–graft - geometry B with a total of 66 cells and 9 rows.

B. Materials of Stent-graft

Nickel-titanium alloys (known as Nitinol), are alloys where this two elements are present in roughly equal atomic

Stepan Major is assistant professor at University of Hradec Kralove, Technical Department, Faculty of Education, Hradec Kralove 500 38, Rokitanskeho 62, Czech republic, stepan.major@uhk.cz.

Marie Hubalovska is Ph.D. student at University of Hradec Kralove, Department of informatics, Faculty of Science, Hradec Kralove 500 38, Rokitanskeho 62, Czech republic, marie.hubalovska@uhk.cz. She works as assistant at Faculty of Education, University of Hradec Kralove from 2014.

percentages. This alloys are characterized by two closely related and unique properties: shape memory and superelasticity. Shape memory is the ability of nitinol to undergo deformation at one temperature, then recover its original, undeformed shape upon heating above its "transformation temperature". Superelasticity occurs at a narrow temperature range just above its transformation temperature; in this case, no heating is necessary to cause the undeformed shape to recover, and the material exhibits enormous elasticity, some 10-30 times that of ordinary metal. This behavior can be explained by changes in crystal structure. At high temperatures, nitinol assumes austenitic structure, which is an interpenetrating simple cubic structure. At low temperatures, nitinol spontaneously transforms to more complicated body-centered tetragonal crystal referred to as martensite.

Mechanical and physical properties of materials were measured in Institute of Material Physic, Academy of Science in Brno. A self-expandable Nitinol stent-grafts repair utilizes these characteristics rather well. Cooled to less than 5 °C (so-called austenite finish temperature), it fully transforms into martensite and hence becomes very deformable and easily compressed into a small catheter. The stents studied in this work were made from two different Nitinol alloys Nitinol-55 and Nitinol-49 (Marked by titanium content) characterized by this mechanical properties.

Young modulus for *Nitinol-55 are*:

- $E_{austenite}$ = 83 GPa
- $E_{martensite}$ = 32 GPa.

Young modulus for *Nitinol-49 are*:

- $E_{austenite}$ = 81 GPa
- $E_{martensite}$ = 41 GPa.

Poisson ratio for both alloys is 0.333. Contrary to conventional engineering materials, Nitinol fracture is not stress based but strain based. Outer packaging referred to as Graft was made from polyethylene terephthalate (PET, also known as Dacron). This material is characterized by Young's modulus is E = 1.2 MPa and a Poisson ratio of 0.495.

C. Stent-graft Function and Loading

Stent-graft has to be placed at the given location (artery, vein, gastrointestinal tube) so as to ensure stent-graft function. Stent is implemented to artery as follows. Stent is cooled first and its dimension are reduced. Then it is inserted into a small catheter and threaded to the delivery system. Reduced stent is loaded into the location. The stent-graft is released from the delivery system via balloon. Stent-graft increases its dimensions when heated to body temperature.

This will provide a passage in the narrow section of artery. Pressure of walls artery prevents expansion of the stent to its original dimensions, causing fixing of the stent at the desired location. This phase is called the sealing phase. Stent has to withstand the pulse of the artery. For example, in the artery the pulsating loading corresponds to the lower and upper pressure value of flowing blood, e.g. diastolic pressure of 50 mmHg (6.3 kPa) and systolic pressure of 150 mmHg (20 kPa).

D. Modeling

1) Geometry modeling

3D-model of stent with a total of 66 bridges or cells and 11 rings (or rows) built into the tubular stent mash was prepared in the SolidWorks, see figure 1B and figure 3.

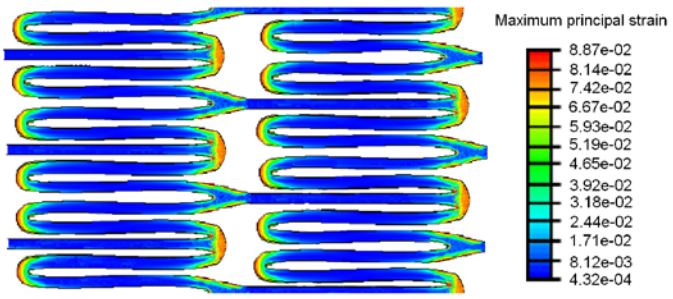

Fig. 3 The maximum principal strain fields in crimpled stent (the stent made from alloy Nitinol-55). The maximum crimping strain (7.8%) is lower under its critical threshold in safe zone.

The model of graft is formed by a thin wall tube. Because stent and graft are sutured together, a tight, rigid contact is assumed to simulate the interaction between stent and graft interaction. Fully expanded stents has a length L of 100 mm, an expanded outer diameter DED of 30 mm, a thickness of 0.44 mm. Although the actual stent-graft comprises eleven rows, it can show that you can use model containing only four rows (24 cells). To verify this assumption, another model was created, which contains only four rows. Other models have been created to describe the unit cell, respectively a bridge. All models were prepared in SolidWorks software and exported in ANSYS software, where they are meshed and solved.

The number of tetrahedral elements of model of whole stent (cut geometry A - F) is presented in table 1. The table also contains a number of tetrahedral elements in the second model, which represents model of only four series cells.

Table 1 The number of tetrahedral elements of model of whole stent

geometry	A	B	C	D
66-cells	892.024	916.048	984.068	884.248
24-cells	389.246	408.024	478.088	418.098

The ANSYS Finite Element Analysis package, in combination with user-defined material subroutines for the Nitinol material properties, was employed to calculate the stress and strain fields. The calculation of stent-graft state under different loadings was based on equation for static equilibrium of the structure(s), where zero body loads were applied:

$$\mathrm{div}(\sigma_{ij}) = 0 \qquad (1)$$

where div(σ_{ij}) is divergence of stress tensor.

The elastic material is characterized by the Lamé constants

μ and λ. On ∂G we impose free-traction boundary conditions, and at infinity the uniform shear stress field is specified.

The displacement field u satisfies the following boundary value problem:

$$\begin{aligned} &\mathrm{div}(\sigma_{ij}) = 0 \nabla.\sigma = 0,\ \sigma = \Gamma : \varepsilon, \\ &\varepsilon = \frac{1}{2}\left(\nabla u + \nabla u^{*}\right),\ x \in B_P / G \\ &\sigma^{(n)}(u;x) = 0,\ x \in B_P / G \\ &\sigma^{(n)}(u;x) = \sigma_{ij}^{\infty} n_j,\ x \in B_P / G \end{aligned} \tag{2}$$

where σ is the stress tensor, ε is the strain tensor, $\Gamma \sim = \{\Gamma ijkl\}$ is the fourth order tensor of elastic constants, (:) denotes contraction by two indices, $B_p = \{(x,y):x2+y\ 2 < p2\}$ and ρ is sufficiently large, n_j are components of the unit outward normal. For an isotropic material which we consider here, the above system is reduced to the Lamé equations:

$$\begin{aligned} &\Lambda(u;x) = \mu \Delta u + \left(\lambda + \mu \nabla \nabla \cdot u\right) = 0, \\ &x \in B_P / G \\ &\sigma^{(n)}(u;x) = 0,\ x \in \partial G \\ &\sigma^{(n)}(u;x) = \sigma_{ij}^{\infty} n_j,\ x \in B_P \end{aligned} \tag{3}$$

Following variational technique, we define the energy space $W(B_P)$ for the boundary value problem (2.2) and introduce the norm:

$$\|u\|_W^2 = \frac{1}{2} \int_{\partial B_P} \sigma_{ij}^{\infty} n_j u_i ds \tag{4}$$

2) Material Modeling

The two materials of the artery wall, arterial tissue and stenotic plaque, were modelled using a 5-parameter third-order Mooney–Rivlin hyperelastic constitutive equation. This has been found to adequately describe the non-linear stress-strain relationship of elastic arterial tissue. The general polynomial form of the strain energy density function in terms of the strain invariants, given by [1, 3] for an isotropic hyperelastic material is:

$$\begin{aligned} W(I_1, I_2, I_3) &= \sum_{i,j,k=0}^{\infty} a_{ijk} (I_1 - 3)^m (I_2 - 3)^n (I_3 - 3)^o \\ a_{000} &= 0 \end{aligned} \tag{5}$$

where W is the strain-energy density function of the hyperelastic material, I_1, I_2 and I_3 are the strain invariants and a_{ijk} are the hyperelastic constants.

Maximum principal strain fields ind crimled stent (The stant made from alloy Nitinol-55). The maximum crimping strain (7.8%) is lower under its critical threshold in safe zone – see figure 3.

III. Mechanics of Stent – Computer Simulation Models

There is number of simulation programs that are based on FEM.

The University of Hradec Kralove is used simulation program *SolidWorks®*. *Solid Works* is a parasolid-based solid modeler, and utilizes a parametric feature-based approach to create models and assemblies [4].

SolidWorks Simulation program is fully integrated into *SolidWorks. SolidWorks Simulation* allow designer verify the model or assembly in terms of its strength and safety.

SolidWork Simulation program has implemented tools, that allow provide steps of process of use of the FEM method. The role of the designer is limited to the first and the second step. Other steps are executed directly by *SolidWorks Simulation* program [4].

A. Displacement of the Stent

Before application of the stent its expanded size is reduced to approximately 1/5 of its diameter. Then the stent is placed to the delivery system. Inducted reaction force against external loading are much larger than the reaction forces in stent-graft. The simplified model of symmetry is used in the stents. The model defines two major directions. The axial direction defines the end node of the stent fixed into the artery. Radial direction defines free radial stent deformation due to external loading caused by crimping tool.

High radial forces can affect the fatigue life of the stent and at the same time can cause breakage of delivery device. It is therefore important to ensure optimum clamping of the stent to the delivery device. Moreover, the emphasis is on ensuring optimum value of the radial force. The maximum main strain fields in the stent after crimping is shown in figure 3. The maximum crimping strain is 7.8% and 10.1% for 55-Nitinol and Nitinol-49.

The radial forces as the function of the displacement simulated by SolidWorks computer simulation program are shown on the figure 4.

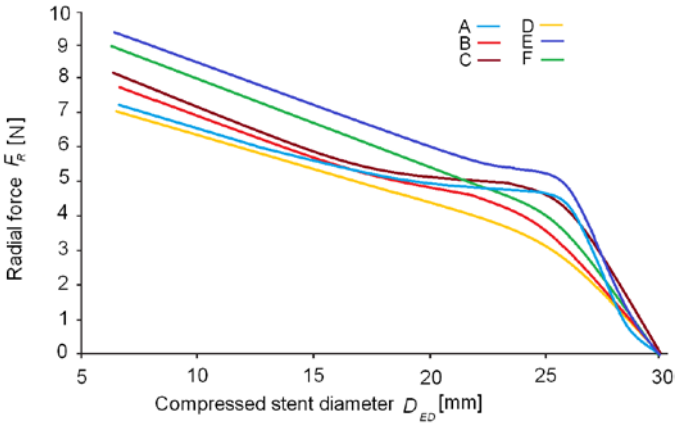

Fig. 4 The radial forces as the function of the displacement. A-F geometry of stent-graft – SolidWorks FEM computer simulation model.

Model of FEM is to be validated. Validation was performed

on the sample of experimental stent. Due to fixing the stent on the measuring device were dimensions of experimental sample two times bigger than the actual size of the stent. The result shown on the figure 4 confirm good agreement between experiment and calculation.

B. *Fixation of the Stent*

Fixation of position in given place of artery is one of the most important assumption. The fixation is given by stent dimensions. The outer radial dimension (diameter) of the stent is approximately 15 - 30% larger than the diameter of the artery. The artery acts by radial force reactions and prevents expansion of the stent to its original size. Between the wall of the artery and stent is formed a contact pressure which prevents movement of the stent in the tube. Analysis of the mechanical response of graft material of stent is negligible.

The stent was mounted to the measurement device in the same manner in which it is fixed in artery, including uniform pressure on the inside part of the arterial wall. The applied pressure corresponds to the value (13 kPa). Radial force is a function of the compressed stent diameter and is shown on figure 5.

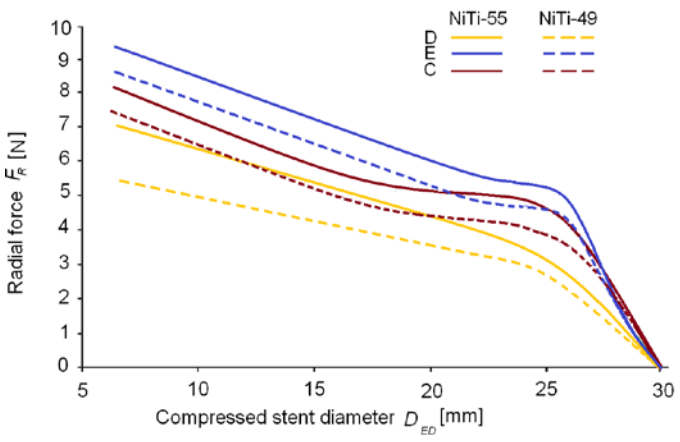

Fig. 5 The radial forces as the function of the compressed stent diameter. A-F geometry of stent-graft – SolidWorks FEM computer simulation model.

The graph shows the radial force and diameter for both alloys. Radial strength is higher for stents made of Nitinol alloy-55. The fatigue life is the most influenced by oscillating strain. The mean strain and stress can be neglected. Therefore, oscillating values of stress / strain Were calculated. These changes of values of stress / strain Were Caused by oscillating pressure in the vessel / artery. The pressure in the artery changed from 50 mmHg it 150mmHg (6.3-20 kPa). The strain changes for one cell are shown in figure 5. The Alternating strain Represents 0.2% of mean strain and safety factor is 2.1 for stents made from Nitinol-55. Alternating strain is 0.24% of mean strain and safety factor is 1.7 for stents made from Nitinol 49.

C. *Fatigue Life of the Stent*

After the deployment of the stent-graft in artery, a major portion of the stent-graft forms new vessel, which excludes the flow of blood from the abdominal cavity of aortic aneurysms. Simulation model of the state used the same boundary conditions identical with crimping and sealing loadings. In addition to the pressing and sealing cyclic arterial pressure by 50 mm Hg (diastolic-6.3 kPa) to 150 mm Hg (systolic-20 kPa) was applied to the inner surface of the graft housing, together with representative intermediate pressure 100 mm Hg (12.7 kPa). FEM shows that the maximum wall stresses 3.4 MPa in the graft, it is much lower than the yield stress of 59.6 MPa. Comparison of experimental measured and SolidWorks simulated fatigue life curves for stent-grafts during cyclic loading are shown on figure 6.

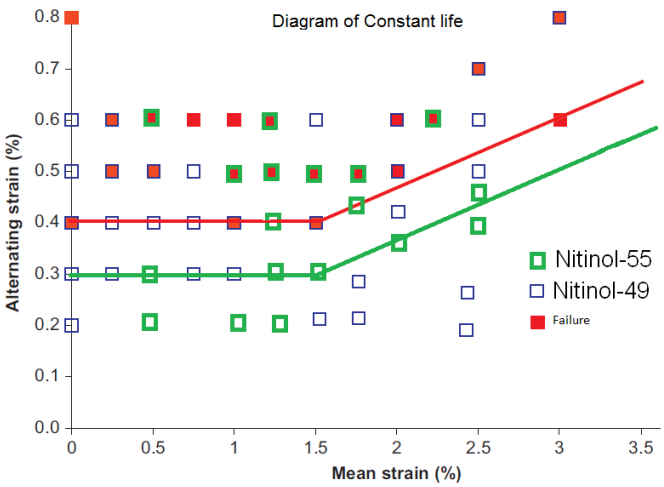

Fig. 6 Comparison of experimental measured and SolidWorks simulated fatigue life curves for stent-grafts during cyclic loading.

IV. Conclusion

As shown in the paper, modeling and computer simulation together with a multidisciplinary approach provides new methodology of experimental research in current sciences.

The result presented in the paper confirms suitability of using of finite element method for computational analysis of mechanical properties of the stent-grafts.

Acknowledgment

This research has been supported by: Specific research project of University of Hradec Kralove, Faculty of Education in 2015.

References

[1] C. Kleinstreuer, Z. Li, C.A. Bascian, S. Seelecke, M.A. Farber, *Journal of Bimechanics*, Volume 41, 2008, 2370–2378.
[2] C. Lally, F. Dolan, P.J. Prendergast, *Journal of Bimechanics*, Volume 38, 2005, 1574–1581.
[3] W. Maurel, Y. Wu, Y., N. Magnenat Thalmann, D. Thalmann, "*Biomechanical Models for Soft-Tissue Simulation*". Springer, Berlin 1998.
[4] S. Hubalovsky, "Modeling, Simulation and Visualization of static Mechanical Properties of Frame of Elevator Cab". *International Journal of Mathematical Models and Methods in Applied Sciences*. 2013, Vol. 7, No. 6, p. 666-675.